

Investigation of deformation principle during hybrid process of laser quenching and forming based on in-situ deformation monitor

Yuki MANABE^{1, a *}, Hiromichi NISHIDA^{1, b}, Tomonao HIROTA^{1, c},
Toshiki HIROGAKI^{1, d}, Eiichi AOYAMA^{1, e}, and Keiji OGAWA^{2, f}

¹Graduate School of Science and Engineering, Doshisha University,
1-3, Tataramiyakodani, Kyotanabe, Kyoto 610-0394, Japan

² Graduate School of Engineering, Ryukoku University,
67, Fukakusa Tsukamoto, Fushimi, Kyoto, Kyoto612-8577, Japan

^ay.manabe.dss@gmail.com, ^bhiromichi0917@gmail.com, ^cdupbuj@gmail.com,
^dthirogak@mail.doshisha.ac.jp, ^eeaoyama@mail.doshisha.ac.jp, ^fogawa@rins.ryukoku.ac.jp

Keywords: laser quenching; laser forming, in-situ monitor

Abstract. In recent years, product miniaturisation and multifunctionalisation have progressed while the importance of process consolidation has increased. This paper examines processes involving the use of a laser to treat and mould small components. Based on consistencies between the laser quenching and forming processes, laser quenching-forming has been proposed as a combination method. Whereas conventional laser forming involves the use of a temperature gradient mechanism, laser quenching-forming often requires the use of a buckling mechanism. The deformation behaviour of the buckling and temperature gradient mechanisms during laser irradiation are analysed in an attempt to better understand these mechanisms. In addition, a measure to control buckling during laser scanning is proposed.

Introduction

The miniaturisation and multifunctionalisation of products such as mobile phones has been accompanied by a reduction in the size and an increase in the complexity of product components. The processing steps used to manufacture such components include rough machining, surface finishing, drilling, heat treatment, etc., and the variety of processing machines has increased with the need to introduce new processes. At the same time, the importance of reducing time and saving space under process consolidation has also increased. However, the processing time required in the press forming and heat treatment steps has not been successfully reduced for smaller components, and in fact problems with increased power consumption and reduced time efficiency have appeared as component sizes decrease. In general, the processing of a small part requires the use of a processing method commensurate with the size of the part, and approaches to this problem have led to the downsizing of production and the implementation of cell production systems[1]. In line with these developments, laser processing has drawn attention as a space-saving method [2].

Heat treatment using lasers has been studied for many years and has led to practical applications such as key groove quenching [3]. Laser quenching has advantages in terms of enabling local quenching and requiring no coolant. Similarly, laser forming has been actively studied in recent years in applications involving the production of thin aluminium and titanium plates [4]. The laser forming process has advantages in terms of high bending accuracy and the lack of a need for metal moulding. As the processing time of laser-based methods depends on

the size of the object to be processed, both laser quenching and forming are better suited than conventional heat treatment and moulding methods to the processing of small products.

Based on consistencies between the working processes of laser quenching and forming, this paper focusses on the laser quenching-forming method combining the two processes. Using this hybrid approach, the process of small thin-plate manufacturing becomes both faster and more efficient. Previous studies examined conventional problems of deformation, hardness, and power consumption in laser scanning and demonstrated that laser scanning from the upper and lower surfaces of a thin plate can be used to carry out both full-thickness quenching and laser forming [5]. In conventional laser forming, deformation can generally be achieved through a relatively controllable temperature gradient mechanism. By contrast, laser quenching-based forming techniques often use relatively small laser scanning speeds to reach the quenching depth, creating a condition in which the temperature gradient and buckling mechanisms coexist.

In this study, the deformation behaviour of a workpiece during laser quenching-forming was analysed with the goal of determining the temperature gradient and buckling mechanisms from the deformation behaviour during laser scanning. In addition, a method for controlling deformation in the presence of a buckling mechanism was investigated.

Concept and Basic theory

Laser quenching and forming hybrid method. Figure 1 shows the proposed a laser quenching and forming hybrid method for thin carbon steel plate (thickness 0.5mm, size 30x30mm) with a 30W small power diode laser. This method makes it feasible to perform both hardening in entire depth direction of plate and forming at the same time, and is considered to be effective to manufacture various kinds of flat spring of complex shape. However, a problem has emerged that there is a complicated phenomenon during laser irradiation because both thermal stress and transformation stress occur at the same time. We therefore attempt to monitor the deformation behavior during laser irradiation in-situ monitor with a video record.

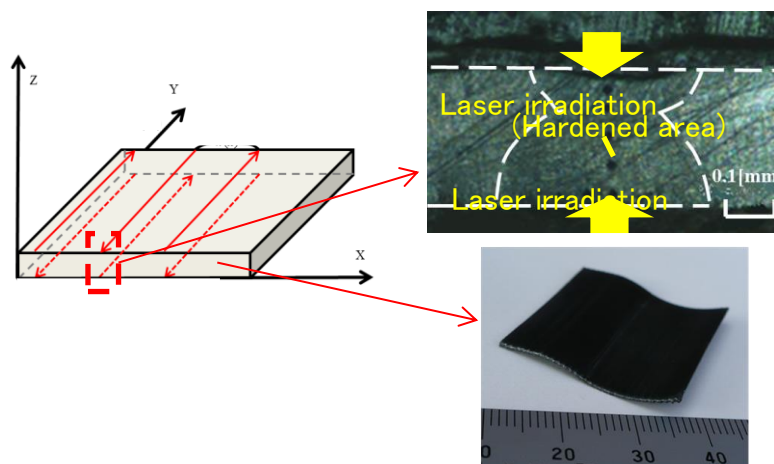
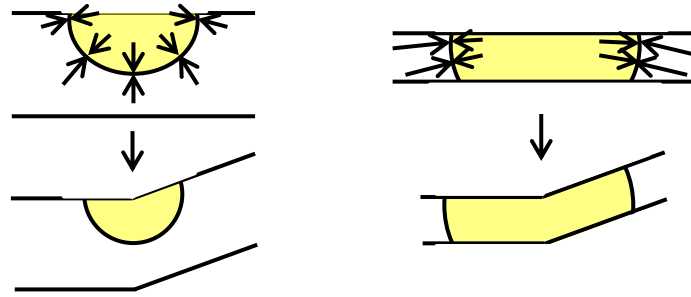


Fig. 1 Proposed laser-forming method

Principles of laser-forming deformation. The temperature gradient mechanism (TGM) is the deformation occurring just below the point of laser irradiation as a result of the temperature gradient created by the irradiation (**Fig. 2(a)**) [6]. In this process, the surface of the test piece in the vicinity of the irradiation receives a compression stress, with the compression of the

irradiated surface determining the direction of deformation. Under these circumstances, deformation control is easy, and TGM is therefore generally used in laser-forming deformation.

In the buckling mechanism (BM), which is illustrated in Fig. 2(b), compressive stress from thermal expansion results in a process similar to buckling. Because the temperature gradient during laser irradiation is almost uniformly distributed on each side of the irradiation point, the direction of deformation largely depends on the initial disturbance [7]. Under the BM, deformations larger than those under TGM are easily obtained. As the controllability of the buckling process is poor, BM is generally avoided in general laser forming; however, when laser quenching and forming are performed at the same time, scanning under BM conditions might be required to attain a specific hardening depth.



(a)Temperature gradation mechanism (b)Buckling mechanism

Fig. 2 Laser-forming mechanisms

Prediction of temperature distribution. Thermal cameras can only observe the temperature of the facing side of a body. Therefore, to model the thermal dynamics in the experimental workpiece, a Gaussian distribution-based prediction equation of the temperature increase in a semi-infinite body irradiated by a moving heat source was used. For the calculations, a coordinate system centred on the scanning centre of the laser spot on the test piece (in which the thickness direction of the test piece was $-z$ and the laser scanning direction $+y$) was used. Because a finite plate thickness was assumed, the image method could be applied to the results in the thickness direction to model the temperature inside the test piece [8]. The moment image method, which is used to model the influence of edges, was used to calculate the energy distribution under the assumption of constant energy input to the inside of the system by folding the energy at the edge and then superimposing the folded energy [9]. An example of the temperature distribution obtained from energy input to an infinite body is shown by the solid line in Fig. 3. As the actual thickness of the workpiece is finite (0.5 mm), the energy is folded back, as shown by the black broken line in the figure, while the total temperature distribution derived in this iteration is indicated by the red dot-chain line. By repeating this superimposition, the input energy to an infinite body can be fitted to a finite field. The equation for estimating the temperature increase in a semi-infinite body from a moving heat source with a Gaussian distribution is given as

$$T_v(x, y, z, \infty) = \frac{2\varepsilon P\sqrt{\kappa}}{\pi^{2/3}K} \int_0^\infty \frac{1}{\sqrt{\tau}(8\kappa\tau + r_0^2)} \times \text{Exp}\left[-\frac{2(x + v\tau)^2 + 2y^2}{8\kappa\tau + r_0^2} - \frac{z^2}{4\kappa\tau}\right] d\tau \quad (1)$$

where P is the laser output [W], ε is the absorptance, r_0 is the irradiation radius [mm], κ is the thermal diffusivity [m^2 / s], K is the thermal conductivity [$\text{W} / (\text{m} \cdot \text{K})$], and v is the feed rate [mm / min] [10][11].

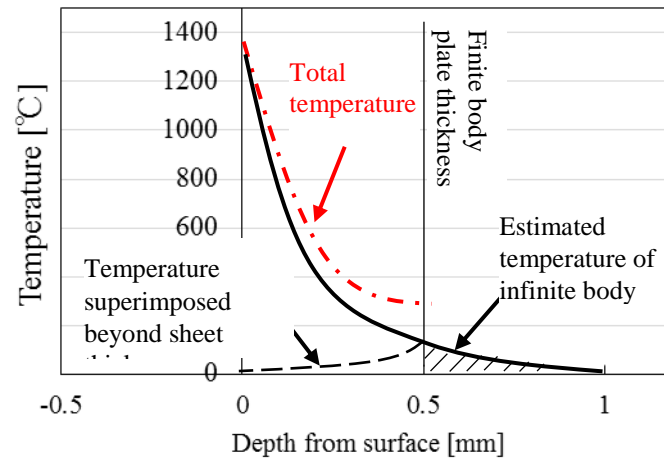


Fig. 3 Foldback of heating at the test piece edge using thermal imaging method

Determination of feed speed

Discrimination of deformation principle. To reliably determine which feed speed regions can be respectively attributed to the BM and the TGM, the relationship between the feed speed and the deformation angle after laser irradiation was investigated. In the results shown in **Fig. 4**, the deformation angle has a local maximum value. As the BM can generally produce a larger deformation angle than the TGM, we assume that this maximum can be attributed primarily to the BM. The figure also shows that the deformation angle becomes very small after exceeding the local maximum, suggesting an immediate transition to the TGM. Correspondingly, we considered a BM occurring in the vicinity of the maximum value and a TGM at a feed speed of about four times the local maximum value. Using Eq. 1, isothermal diagrams for the feed speeds corresponding to the hypothesised BM and TGM points were obtained (**Figs. 5** and **6**, respectively). It is seen from Fig. 5 that, at the feed speed corresponding to the conjectured BM, high temperature regions are distributed toward the lower side of the workpiece. From Fig. 6, it is seen that the high temperature regions are limited to the vicinity of the laser irradiation surface at the feed speeds corresponding to the conjectured TGM.

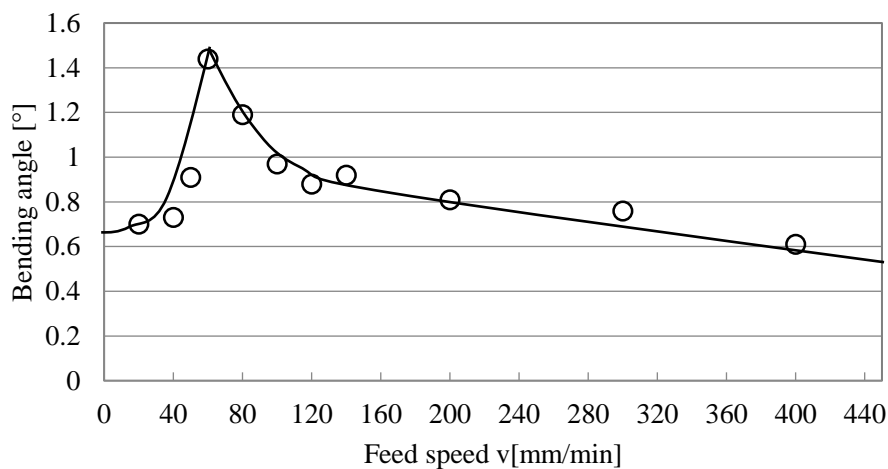


Fig. 4 Relationship between feed speed and bending angle after laser irradiation

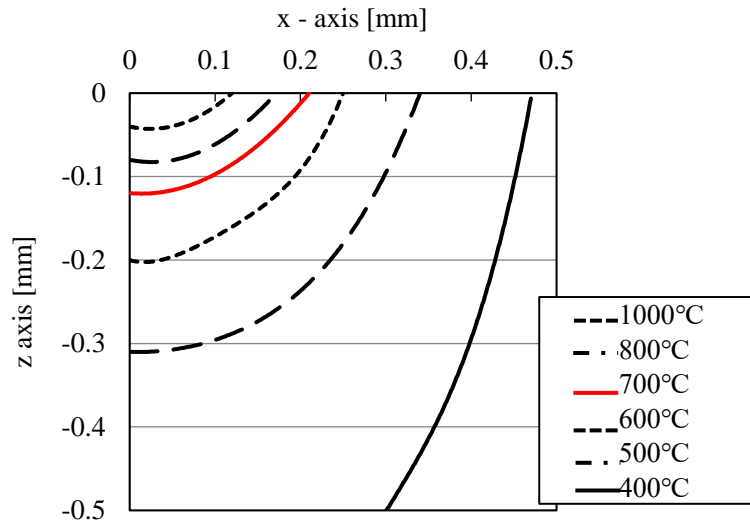


Fig. 5 Isothermal diagramat hypothesised BM (80 mm/min)

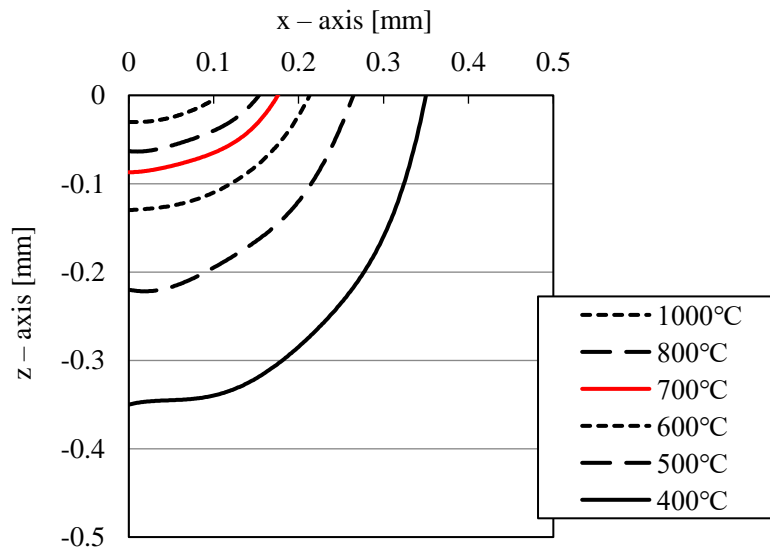


Fig. 6 Isothermal diagram at hypothesised TGM (300 mm/min)

In-situ confirmation of deformation principle with a video record. To confirm the BM and TGM deformation principles hypothesised in Section 3.1 above, the deformation behaviour during laser irradiation was investigated using the following setup and methods.

To investigate the deformation behaviour during laser irradiation, observations of one end of the workpiece were carried out with recoding a video image as it expanded from the treatment. As shown in Fig. 7, the deformation angle was calculated by observing the displacement of the end of a carbon rodplaced at the end of the test piece.

Under BM, features similar to buckling should appear; therefore, the presence of the BM should be deducible from the rapid appearance of buckling.

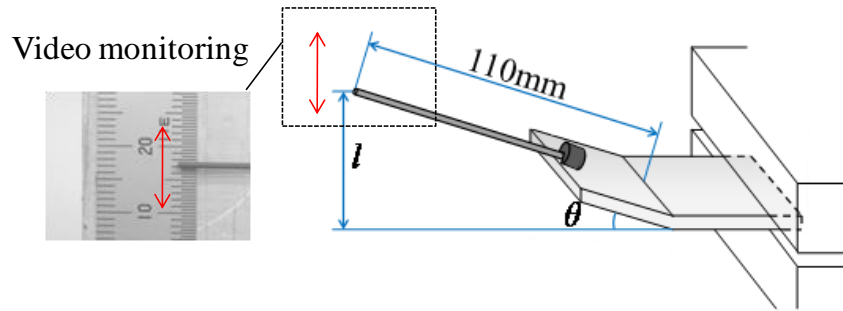


Fig. 7 Vertical displacement from deformation l

Experimental conditions

The laser used in the experiment was a small-output semiconductor laser (LD-HEATER L 10060; Hamamatsu Photonics) with an output and spot diameter of 30 W and 0.4 mm, respectively. A 30×30 mm piece of S55C steel, which has a sufficient amount of carbon for quenching, was used as a workpiece. The full specifications and conditions of the laser and workpiece and the physical properties of the S55C steel used in the experiment are listed in **Tables 1** and **2**, respectively.

Table1 Experimental conditions

Laser	Output power	30 W
	Spot diameter	0.4 mm
	Wavelength	808 nm
	Defocus length	0.0 mm
	Cooling method	Air cooling
Workpiece	Material	S55C
	Carbon content	0.53%
	Hardness	180–200 HV
	Size	30×30 mm
	thickness	0.5 mm

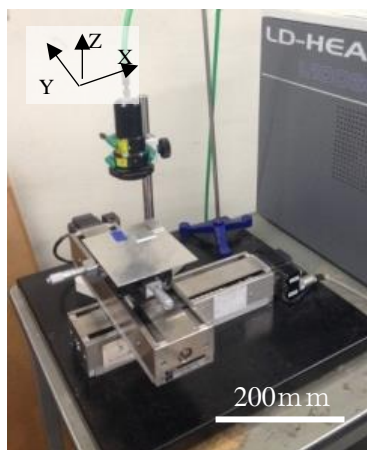
Table 2 Properties of S55C

Density	$7,860 \text{ kg/m}^3$
Longitudinal elastic modulus	$208 \times 10^{11} \text{ Pa}$
Poisson's ratio	0.3
Coefficient of linear expansion	$11.6 \times 10^{-6} \text{ 1/K}$
Specific heat	$435 \text{ J/kg} \cdot \text{K}$
Thermal conductivity	$46.5 \text{ W/m} \cdot \text{K}$

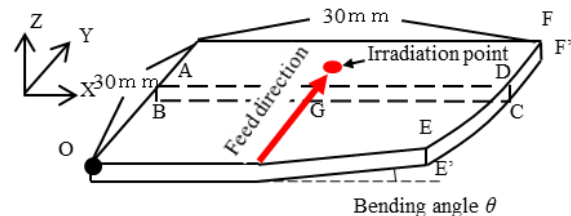
The workpiece was placed on the XY table shown in **Fig. 8 (a)** and the feed speed was controlled using a function generator. The experimental condition during laser scanning is shown in Fig. 8 (b)(c), in which the coordinate system with origin at point O is defined as X - Y - Z (although not shown in the figure, the coordinate system with the laser irradiation point as the origin is defined as x - y - z). Under the assumption of heat dissipation from natural convection into the atmosphere, the experimental condition could assume minimised

disturbance from solid heat transfer within the fixed part. Sides E–F and E–F' on the front and back, respectively, of the test piece were fixed from the top and bottom ($\pm Z$ -directions) with heat insulating ceramics.

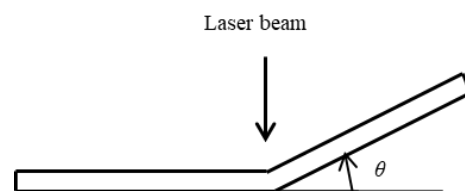
In the laser-forming process, defocussing is often carried out to avoid surface melting; in laser-quenching-forming, however, defocussing can lead to significant deterioration of quenching performance. Correspondingly, the defocus distance in the experiments was set to zero.



(a) Experimental setup



(b) Scanning condition



(c) Bending angle θ

Fig. 8 Laser processing conditions

Result and discussion

Single laser scanning. The deformation behaviours occurring in the workpiece under laser scanning at feed speeds of 80 (BM) and 300 mm/min (TGM) are shown in **Figs. 9.** and **10,** respectively. In each figure, it is seen that all parts of the workpiece are deformed, even in regions in which no laser irradiation is performed, although in each case the piece is seen to be slightly compliant, displaying a gradual change in deformation with distance from the laser irradiation position. This pattern possibly occurs because the workpiece cannot be deformed in a purely localised fashion but must bend in a manner that affects the overall specimen.

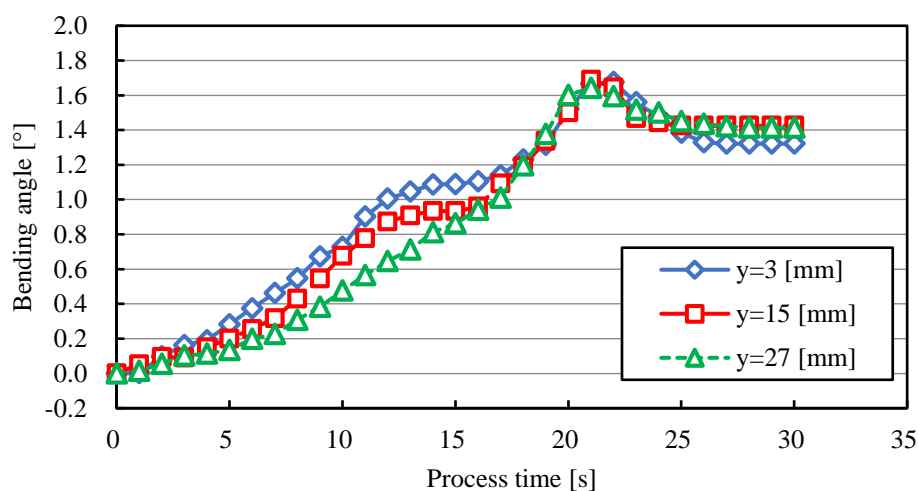


Fig. 9 Bending behaviour without initial scan (80 mm/min)

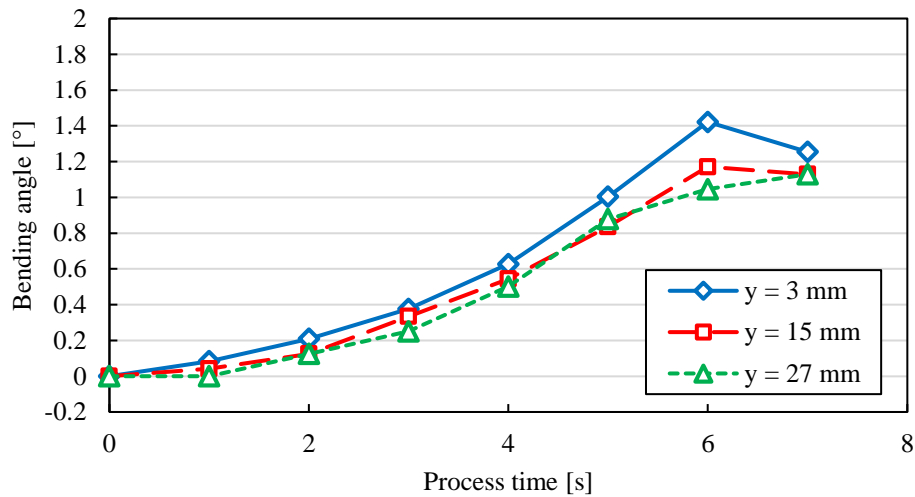


Fig. 10 Bending behaviour without initial scan (300 mm/min)

To further understand these effects, the respective forces that promote and prevent deformation must be considered. In the former case, the laser-irradiated region is deformed under compressive stress, resulting in a slight deformation in the non-irradiated regions. The force promoting deformation increases with time, reaching a maximum at the cessation of irradiation. In the latter case, the non-irradiated regions play a role in preventing deformation; thus, as the irradiated spot position changes during the laser scanning process, the force hindering deformation is locally removed. The hindering force therefore decreases with time, reaching a minimum value upon cessation of laser irradiation. In Fig. 9, the piece is deformed in a nearly linear manner and does not undergo any short-duration large deformation; thus, it cannot be considered to experience complete buckling. By contrast, Fig. 10 shows a change that can be plotted using a simple quadratic function, suggesting that a deformation-preventing force has transitioned to a deformation-enhancing force.

The deformation behaviour seen in the previous results alone could not confirm the presence of the BM. Therefore, the behaviour from 10–15 s in Fig. 9 was analysed more closely. Following a stagnation during this period, the figure seems to indicate the occurrence of a large deformation from 15–20 s. The smaller disturbance at the beginning of the experiment suggests TGM features appearing at the beginning of the laser scanning process. In the second half of the scanning process, disturbances from residual stress or deformation occur, suggesting the appearance of strong BM features. Therefore, prior to examining the deformation behaviour, laser scanning was performed from the back side of the piece at a feed speed of 100 mm/min; the results were then measured at a feed speed of 80 mm/min (Fig. 11). Comparison of the results with those in Fig. 9 show a clear loss of linearity and an emphasis of features causing large deformation within a short time frame. Furthermore, whereas the results in Fig. 9 show features of gradual deformation from the laser irradiation spot, no such features are seen in Fig. 11, suggesting nearly simultaneous deformation—a feature generally seen under buckling. These results strongly suggest deformation as a result of the BM at a feed speed of 80 mm/min. Although linear deformation behaviour appears to rule out the presence of the BM, in cases of extremely small disturbances TGM characteristics can appear more prominently than BM characteristics, making it necessary to apply an initial disturbance to perform discrimination under the deformation principle.

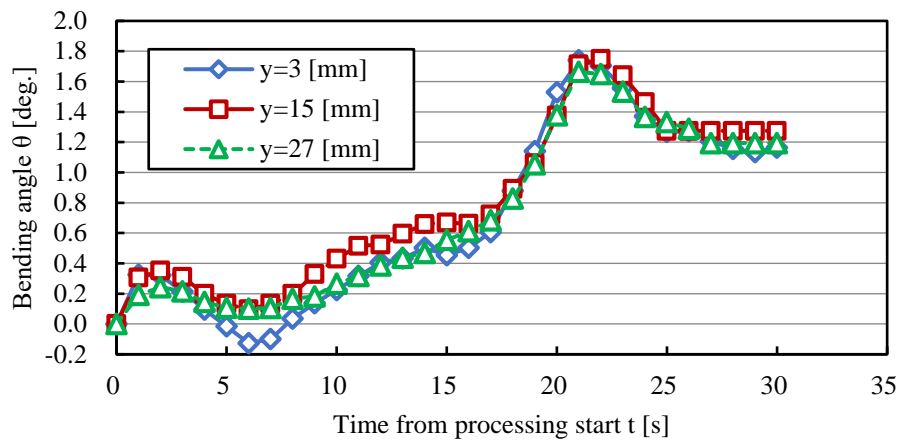


Fig. 11 Bending behaviour following initial scan (1 scan, 80 mm/min)

Laser scanning with initial deformation. In the previous section, it was shown that prominent BM features can appear following even a small initial disturbance from one laser scan. This suggests that increasing the size of the initial disturbance can result in the appearance of stronger BM characteristics. To test this, the deformation behaviour under larger initial disturbances from advance laser scanning was investigated. The laser was scanned over the entire surface of one side of the specimen at a feed rate of 100 mm / min in the manner shown in **Fig. 12**.

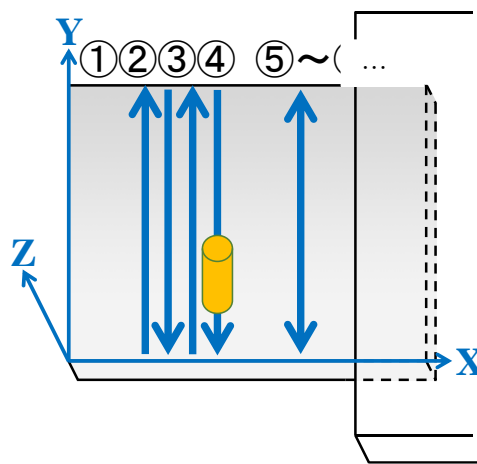


Fig. 12 Area scanning for initial disturbance

The resulting initial disturbance produced a residual stress about 10 MPa and a curvature radius of about 30 mm. The piece was then scanned at feed speeds of 80 mm/min, which produced both negative and positive deformations, as shown in **Figs. 13** and **14.**, respectively. The deformation behaviour at a feed rate of 300 mm/min was then analysed, with the results shown in **Fig. 15**. Although the directions of deformation are opposite, the results in Figs. 13 and 14 show practically identical deformation behaviour. In each case, a large deformation occurs just after the beginning of laser scanning; once this has stabilised, another large deformation in the opposite direction returns the piece to its original state. A potential explanation for this behaviour lies in the fact that the forces promoting deformation at the scanning starting and ending points are small, with the workpiece deforming between 5–15 s from the start of the scanning process but not before or after. This suggests the presence of a force preventing

deformation during the early and later stages of scanning, and therefore that both the beginning and end of the process represent fixed states, resulting in a stabilization at zero deformation. Furthermore, none of the linearity described in Section 5.1 is observed, indicating that the deformation behaviour is complicated by the initial disturbance. However, examination of the bending behaviour in Fig. 10, which is attributable to the TGM, reveals strong linearity despite the presence of an initial disturbance. Although the final deformation angle decreases slightly under the influence of various deformation-inhibiting factors, the controllability can be considered to be relatively good, with no extreme decrease in deformation of the type that would be expected in the presence of the BM. The improved controllability of the TGM appears to stem from the stability of the deformation direction. In laser forming using laser scanning, the entire test piece must be balanced and, therefore, when even a local stress is applied in a direction differing from that of deformation, it will exert a pull on the surrounding material. On the other hand, under the TGM, in which compression in a single direction occurs, stress-induced deformation results in increased expansion in the surroundings, resulting in a simpler pattern of deformation.

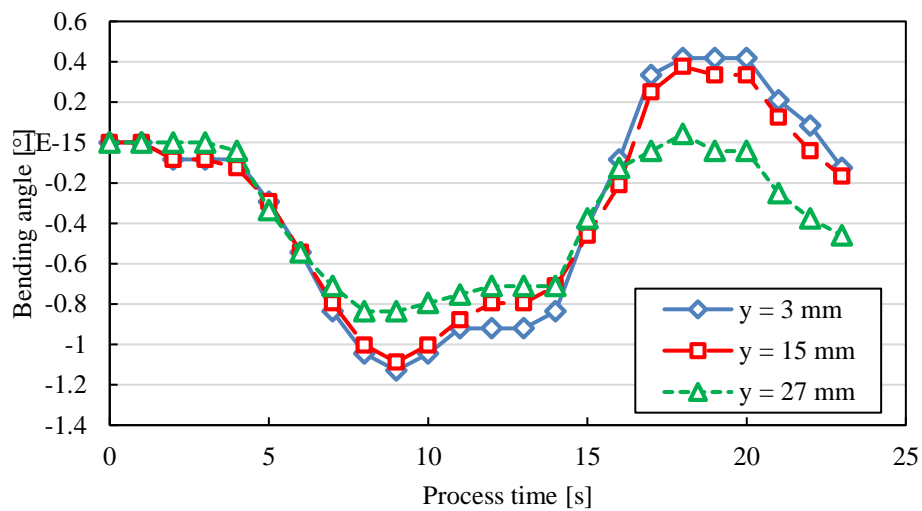


Fig. 13 Bending behaviour following initial scan (area scan, 80 mm/min, negative)

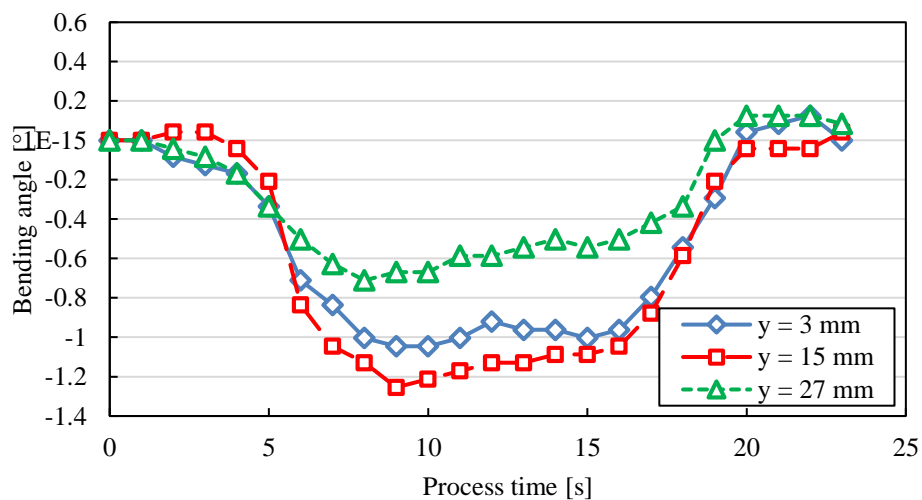


Fig. 14 Bending behaviour following initial scan (area scan, 80 mm/min, positive)

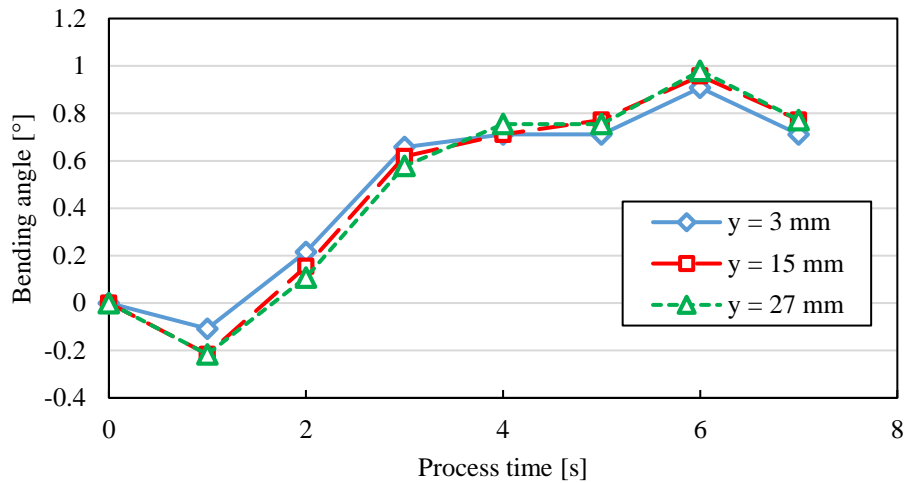


Fig. 15 Bending behaviour following initial scan (area scan, 300 mm/min)

From the above results, it can be concluded that, under the application of laser scanning to both the upper and lower surfaces of a piece, the BM governs neither positive nor negative deformation behaviour and there is a reduced amount of deformation. On the other hand, the bending seen in Fig. 11, in which the external disturbance is suppressed to a relatively small level, maintains a somewhat gauge linearity and suggests a certain level of controllability. This suggests that, under two-sided planar laser quenching, deformation control can be maintained by alternately scanning the upper and lower sides to avoid the occurrence of the BM.

Conclusion

In this study, the deformation behaviour of the TGM and BM under laser quenching-forming was analysed. The results are summarised as follows.

- 1) When the initial disturbance is small, both the BM and the TGM exhibit very similar deformation behaviours.
- 2) When the initial disturbance increases, the BM cannot maintain linear deformation, resulting in a large degree of deformation within a short time frame.
- 3) When laser quenching-forming is performed over an area, it is necessary to select the order in which the initial disturbance is minimised.

References

- [1] Y. Okazaki, T. Mori, N. Morita., Desk-top NC milling machine with 200 krpm spindle, Proc. 2001 ASPE Annual Meeting (2001)192-195 (In Japanese)
- [2] A.K. Dubey, V. Yadava, Laser beam machining: a review, International Journal of Machine Tool and Manufacture, Vol. 48 (2008) 609-628
- [3] H.G. Wang, Y.H. Guan, T.L. Chen, J.T. Zhang, A study of thermal stresses during laser quenching, Journal of Materials Processing Technology, Vol. 63 (1997)550-553
- [4] E.C. Santos, M. Shiomi, K. Osakada, T. Laoui, Rapid manufacturing of metal components by laser forming, International Journal of Machine Tools & Manufacture, Vol. 46 (2006)1459-1468
- [5] Y. Manabe, R. Oda, T. Hirogaki, E. Aoyama, K. Ogawa, Whole Quenching of Small Thin Plate with Low-Power Semiconductor Laser Based on Feed-Speed Combination Problem, International journal of automation technology, Vol. 10 (2016) 923-933
- [6] H. Shen, Y. Shi, Z. Yao, J. Hu, An analytical model for estimating deformation in laser forming, Computational Materials Science, Volume 37 (2006) 593-598
- [7] F Vollertsen, I Komel, R Kals, The laser bending of steel foils for microparts by the buckling mechanism-a model, Modelling and Simulation in Materials Science and Engineering, Volume 3 (1995) 107-119
- [8] T, Hirogaki, H. Nakagawa, M. Hayamizu, Y. Kita, Y. Kakino, I. Yamaji, Heat Treatment of on-the-Machine Tools using YAG Laser Source : Heat Treatment on the Edge of a Die, Journal of JSPE, Vol. 67, No. 5 (2001) 808-813 (In Japanese)
- [9] K. Umezawa, The Meshing Test on Helical Gears under Load Transmission : 2nd Report, The Approximate Formula for Bending-Moment Distribution of Gear Tooth, Transactions of the Japan Society of Mechanical Engineers, Vol. 38, No. 310(1972) 1602–1608 (In Japanese)
- [10] O. Manca, B. Morrone, V. Naso Quasi-steady-state three dimensional temperature distribution induced by a moving circular Gaussian heat source in a finite depth solid, International Journal of Heat and Mass Transfer, Vol. 38 (1995) 1305–1315
- [11] Y. Namba, E. Ohmura, S. Makinouchi, A Study on Laser Hardening : 2nd Report, Analysis of Hardening Process, Transactions of the Japan Society of Mechanical Engineers Series C, Vol. 50, No. 454 (1984) 1099-1106